# An exercise in forecasting loop current and eddy frontal positions in the Gulf of Mexico

L.-Y. Oey,[1] T. Ezer,[1] G. Forristall,[2] C. Cooper,[3] S. DiMarco,[4] and S. Fan[5]

Received 15 April 2005; revised 23 May 2005; accepted 27 May 2005; published 30 June 2005.

[1] As part of a model-evaluation exercise to forecast Loop Current and Loop Current eddy frontal positions in the Gulf of Mexico, the Princeton Regional Ocean Forecast System (PROFS) is tested to forecast 14 4-week periods Aug/25/99–Sep/20/00, during which a powerful eddy, Eddy Juggernaut (Eddy-J) separated from the Loop Current and propagated southwestward. To initialize each forecast, PROFS assimilates satellite sea surface height (SSH) anomaly and temperature (SST) by projecting them into subsurface density using a surface/subsurface correlation that is a function of the satellite SSH anomaly. The closest distances of the forecast fronts from seven fixed stations in the northern Gulf over a 4-week forecast horizon are then compared against frontal observations derived primarily from drifters. Model forecasts beat persistence and the major source of error is found to be due to the initial hindcast fields. **Citation:** Oey, L.-Y., T. Ezer, G. Forristall, C. Cooper, S. DiMarco, and S. Fan (2005), An exercise in forecasting loop current and eddy frontal positions in the Gulf of Mexico, *Geophys. Res. Lett.*, *32*, L12611, doi:10.1029/2005GL023253.

## 1. Introduction

[2] The Loop Current is the dominant feature of the circulation in the eastern Gulf of Mexico and the formation region of the Florida Current-Gulf Stream system. The Loop Current episodically sheds warm-core eddies or rings that generally translate westward at $2 \sim 5$ km day$^{-1}$, with intense currents $\approx 1.7 \sim 2$ m s$^{-1}$ [e.g., *Elliott*, 1982; *Cooper et al.*, 1990; *Forristall et al.*, 1992]. Smaller eddies (of both signs) exist and there is also considerable interaction between the Loop Current, rings and topography [*Vukovich and Maul*, 1985; *Vidal et al.*, 1992; *Biggs et al.*, 1996; *Hamilton et al.*, 2002]. Models have shown that smaller eddies can affect the behaviors of rings and the Loop Current [*Welsh and Inoue*, 2000], making these features challenging to describe, understand and predict.

[3] As the production of hydrocarbons moved offshore into deeper waters, there is interest to evaluate (and improve) forecast models that track frontal positions associated with the Loop Current and rings. Deepstar Joint Industry Project recently organized such a model evaluation study. Besides PROFS, other models were also tested: CUPOM (Colorado University version of the Princeton Ocean Model; http://e450.colorado.edu), HYCOM (HYbrid Coordinate Ocean Model; http://hycom.rsmas.miami.edu/), NCOM (Navy Coastal Ocean Model; http://www7320.nrlssc.navy.mil/IASNFS_WWW/) and PDOM (Princeton Dynalysis Ocean Model; http://128.160.23.41/Products/modeling/pdom). In this work, we report results from PROFS.

[4] The study consists of 14 4-week test-forecasts (Table 1; Figure 1). Eddy-J separated from the Loop Current around mid-Oct/1999, interacted with the Loop Current and other smaller eddies, propagated southwestward and eventually decayed. As a measure of forecast skill, we compare the shortest distances from either the (forecast) Loop Current or Eddy-J front to the seven sites shown in Figure 1 against the corresponding distances obtained from EddyWatch observations (described below). The forecast was 'blind' in that, although the modelers assimilated satellite data to initialize the forecast, they had no prior knowledge of EddyWatch frontal positions. This procedure is different from previous evaluations of forecast models [e.g., *Ezer et al.*, 1992; *Willems et al.*, 1994] which were all initialized with, and then compared against, the same observation dataset.

[5] Section 2 presents PROFS, section 3 defines frontal positions, section 4 compares forecasts with observations and section 5 concludes the paper.

## 2. Princeton Regional Ocean Forecast System: PROFS

[6] PROFS is based on the Princeton Ocean Model (POM [*Blumberg and Mellor*, 1987]) and has been tested extensively [e.g., *Oey et al.*, 2003; *Fan et al.*, 2004, and references therein]. PROFS uses orthogonal curvilinear grid in the domain 6°–50°N and 55°–98°W. There are 25 *sigma levels* in the vertical; in the Gulf of Mexico the mesh size $\approx$10 km. At 55°W, transports and monthly climatology are specified together with a combination of radiation and advection. All fluxes are zero at closed boundaries. At the sea-surface, six-hourly ECMWF (European Centre for Medium Range Weather Forecast) wind stresses and climatological heat and salt fluxes are specified.

[7] The model's initial state prior to each of the 14 forecast experiments is estimated by assimilating satellite SSH anomaly and SST. *Fan et al.*'s [2004] fields (satellite data-assimilated hindcast since 1992) 15 days prior to each forecast are used to initialize a 15-day hindcast run that assimilates only the satellite data prior to the forecast start date. The SST assimilation uses weekly satellite SST. However, SST tends not to relate to subsurface dynamics, and is not a sensitive parameter for assimilation outside the shelves [*Fan et al.*, 2004].

[1]Department of Atmospheric and Oceanic Sciences, Princeton University, Princeton, New Jersey, USA.
[2]Forristall Ocean Engineering, Inc., Camden, Maine, USA.
[3]Chevron-Texaco, San Ramon, California, USA.
[4]Department of Oceanography, Texas A&M University, College Station, Texas, USA.
[5]Stevens Institute of Technology, Hoboken, New Jersey, USA.


0094-8276/05/2005GL023253

**Table 1.** The 14 Test-Forecast Cases and Periods

| Case# | Start Date | End Date | Case# | Start Date | End Date |
|---|---|---|---|---|---|
| 1 | Aug/25/99 | Sep/22/99 | 8 | Mar/08/00 | Apr/05/00 |
| 2 | Sep/22/99 | Oct/20/99 | 9 | Apr/05/00 | May/03/00 |
| 3 | Oct/20/99 | Nov/17/99 | 10 | May/03/00 | May/31/00 |
| 4 | Nov/17/99 | Dec/15/99 | 11 | May/31/00 | Jun/28/00 |
| 5 | Dec/15/99 | Jan/12/00 | 12 | Jun/28/00 | Jul/26/00 |
| 6 | Jan/12/00 | Feb/09/00 | 13 | Jul/26/00 | Aug/23/00 |
| 7 | Feb/09/00 | Mar/08/00 | 14 | Aug/23/00 | Sep/20/00 |

[8] We use a correlation factor, $F_T$, to project satellite SSH anomaly $\delta\eta_{sa}$ to a temperature-anomaly estimate $\delta T(x, y, z, t) = F_T(x, y, z)\,\delta\eta_{sa}(x, y, t)$ and similarly for $\delta S$ (hence density $\rho$ [*Mellor and Ezer*, 1991]). The $F_T = \langle \delta T\,\delta\eta\rangle/\langle\delta\eta^2\rangle$ is computed from a 10-year ($\langle\rangle$ = time mean) non-assimilated model simulation which produces its own eddy field. An optimum interpolation scheme is then used for assimilation. The $F_T$ is imperfect; so we modify Mellor-Ezer scheme and let $F_{TA}(x, y, z; \varphi) = F_T(x, y, z)[1 + \varepsilon G(\varphi)]$, where $\varepsilon \ll 1$ and G is an O(1) function of the state or forcing variable $\varphi$ (e.g. $\rho$ or $\delta\eta_{sa}$, or some combination thereof). Thus the $F_T$ is assumed to be fairly realistic though it needs to be adjusted for model bias and imperfect physics. The 'G' should ideally be from adequately sampled observations prior to a particular forecast, but this is rarely possible in practice. For the present work, we let $\varphi = \delta\eta_{sa}$ and determine 'G' (actually 'εG') by regressing the *hindcast* $\delta\eta$ against $\delta\eta_{sa}$ for the last 60 days prior to the first test forecast date (Aug/25/1999). This εG is then kept the same for all fourteen test forecasts. A future refinement would be to continually adjust εG prior to a particular forecast using data from the most recent past months, thus producing a slowly-varying correction.

[9] *Walpert et al.* [2004] reported field survey across the Loop Current and Eddy-J near the end of October. Figure 2 compares observed and hindcast currents at $z = -44$ m on Oct/27–29/1999 and Figure 3 vertical-section contours of observed and hindcast temperature along the ship track. There are general agreements including the value and location of maximum speed (indicated as 'X' in Figure 2), though some smaller-scale observed features are missing in the hindcast. In Figure 3, Eddy-J is seen in both observation and model plots as a bowl-shape feature around $x \approx$ 3700 km on Oct/27 $\sim$ 28, and also a smaller feature at $x \approx$ 4200 km between Oct/28 and Oct/29 when the ship returned and passed through the north/northeastern limb of the eddy. The observed eddy is stronger than modeled as seen by the slightly deeper penetration of observed isotherms into the sub-surface. The discrepancy is caused by a general tendency of ocean models to underestimate circulation strengths [e.g., *Oey*, 1998], as well as eddy position errors due to the assimilation scheme and input (satellite) data.

[10] Figure 1 summarizes the behaviors of the Loop Current and Eddy-J. After separation, Eddy-J completed a clockwise rotation from Oct/20 $\sim$ Jan/12 (2.5 months) and at the same time drifted west/southwestward about 270 km (drift speed $\approx$ 4 km/day). The tendency for a Loop Current eddy to rotate clockwise is well-known, though Eddy-J's rotation is slower than for other eddies (e.g. the "Fast Eddy" rotation is about 10 days [*Lewis and Kirwan*, 1987]). In mid-April Eddy-J split into two smaller eddies "*Jn*" and "*Js*" of about equal strengths. Eddy-*Jn* remained in the northwest corner of the Gulf. We track the more variable Eddy-*Js* only. Throughout these periods, the Loop

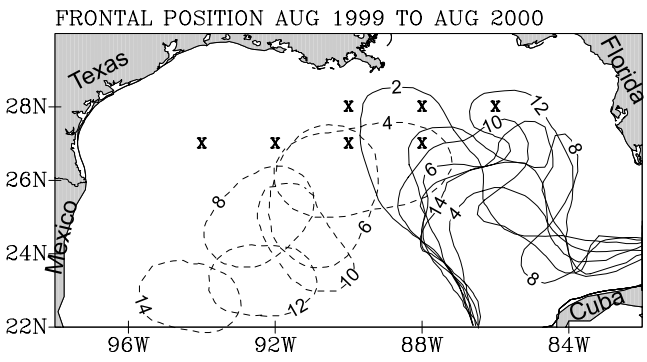


**Figure 1.** Observed frontal positions from Horizon Marine Inc. shown every 8 weeks for the 14 test-forecast periods, beginning with the week-0 of case#2 (Aug/25/99; Table 1). Numbers on contours indicate case #'s. Crosses indicate sites to which closest distances from either Eddy-J (dashes) or Loop Current (solid) front are computed.

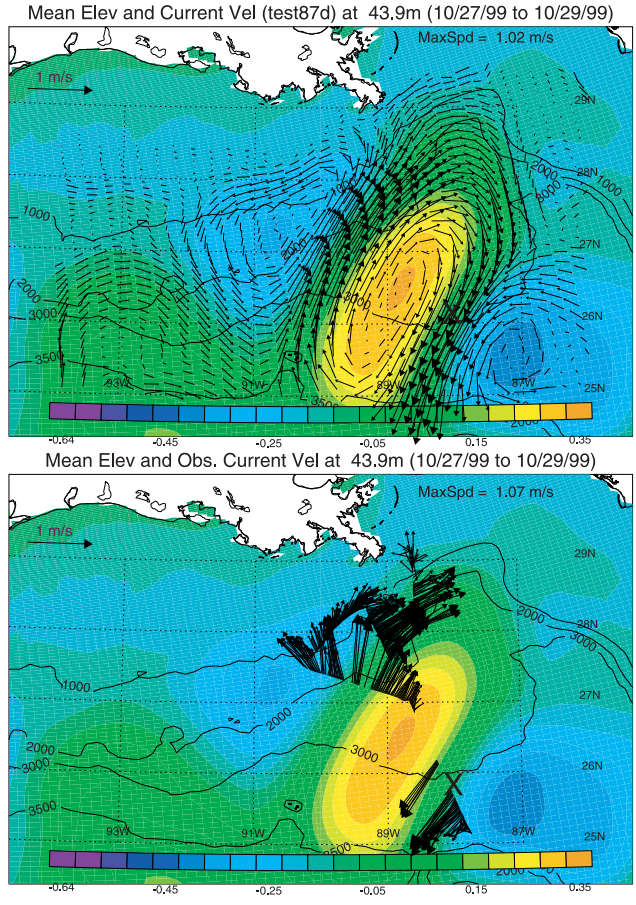


**Figure 2.** A comparison of hindcast currents (upper panel) across Eddy-J with shipboard 38-kHz ADCP estimates of current on Oct/27 $\sim$ 29/1999 at $z = -44$ m. Colors are assimilated SSH in meters (red high and blue low). The dark crosses are maximum speeds and values are printed on top of each panel. Black contours are isobaths in meters.

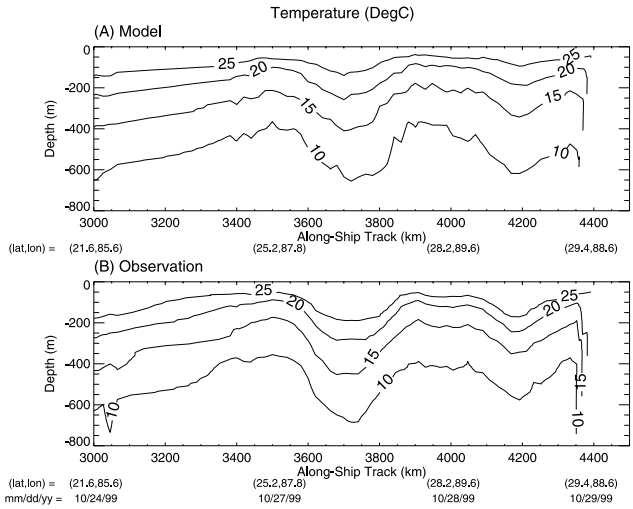


**Figure 3.** Vertical section contours of hindcast (upper panel) and observed temperatures along the TAMU ship-track ($x$-axis) that begins off West Florida shelf ($x \approx 0$), into the Yucatan/Cayman Sea ($x \approx 1000-3000$ km) and then back into the Gulf ($x > 3000$ km as shown). The lat/lon locations of the ship-track are shown under each panel and the corresponding dates are shown under the lower panel. Eddy-J can be seen in both panels around $x \approx 3700$ km on Oct/27∼28.

Current vacillates considerably, e.g. it extended on Aug/25/99 (case#2) and retracted on Jul/26/00 (case#10).

## 3. Frontal Positions and Error Estimate

[11] The observed fronts are from Horizon Marine Inc.'s EddyWatch maps (http://www.horizonmarine.com/ew_descript.html). The maps are from analyses of drifters supplemented by satellite SSH and SST, and some XBT's, and are therefore weighted with surface data. We use the 18°C isotherm at $z = -200$ m to define forecast frontal positions, based on our experience that surface and subsurface fronts are generally correlated. This is reasonable for unbiased model inter-comparisons. However, the positions of surface and subsurface fronts can differ. A simple frontal model based on the conservation of potential vorticity gives a distance-difference $\approx R/2$, subsurface front (at $z = -200$ m) inside the surface front (eddy's depth ≈500 m, c.f. Figure 3), where $R$ is the baroclinic Rossby radius. In the Intra-American Seas, $R \approx 30 \sim 50$ km [*Chelton et al.*, 1998] and the surface-subsurface differences (i.e. the errors) ≈15 ∼ 25 km. *Walpert et al.*'s [2004] data also shows similar surface-subsurface bias. Other types of error (related to differences in surface and sub-surface fronts) also exist, for example, when surface and sub-surface motions are decoupled due to strong (summertime) stratifications. Error estimate in these conditions is beyond the scope of this work.

## 4. Comparison Between Forecast and Observation

[12] As an example, Figure 4 compares forecast (blue) and observation (red) frontal contours for Case 2 (Table 1) when Eddy-J was separating from the Loop Current. The hindcast (green) is also plotted. The forecast correctly predicts the time when Eddy-J separated (Week-3, Oct/13/1999) when both forecast and observed Eddy-J contours cleanly detached from the Loop Current. For hindcast, clean detachment occurred one week later (on Week 4), which suggests the assimilation could be less constrained. Note also that the hindcast and forecast fronts often (but not always) stay inside the observed front – a situation we found occurred 60% of the time through the 14 periods. This is consistent with the surface-subsurface frontal differences discussed previously. After shedding, the model Eddy-J rotated clockwise as observed (Case 3, not shown).

[13] We define model error $E_n = dm_n - do_n$, where $dm_n$ is the shortest distance from either the model Loop Current or Eddy-J front to the site "$n$" and $do_n$ is the corresponding observed distance (Figure 4). The $E$'s and $d$'s are functions of the weekly forecast horizon: four weeks for each of the 14 forecast periods (Table 1). We similarly define persistence error to be $P_n = do_n(\text{week0}) - do_n$, where week0 is the initial time of each of the 14 forecasts. Note that the $P_n$ is with respect to initial observed frontal position which is not assimilated. This definition is stricter than the definition that uses model's initial condition (= hindcast analysis assumed to be the 'observed' [e.g., *Ezer et al.*, 1992]), which would give $E_n = P_n = 0$ at week0. From a practical standpoint, $P_n$ gives error estimate in the absence of a reliable forecast model. Statistics (e.g. root mean squares $RMS$) of $E_n$ will initially indicate larger errors than $P_n(\text{week0}) = 0$, but a useful forecast should show smaller errors at later times. We examined $E_n$ and $P_n$ as functions of the forecast horizon and sites, and derived various statistics. Figure 5 gives a summary based on averages (denoted by $\langle\rangle$) of $E_n$ and $P_n$ over all 14 periods and all sites ($n = 1, 2, \ldots 7$), as well as the corresponding $RMS(E_n)$ and $RMS(P_n)$ respectively. These statistics give an overall measure of the forecast

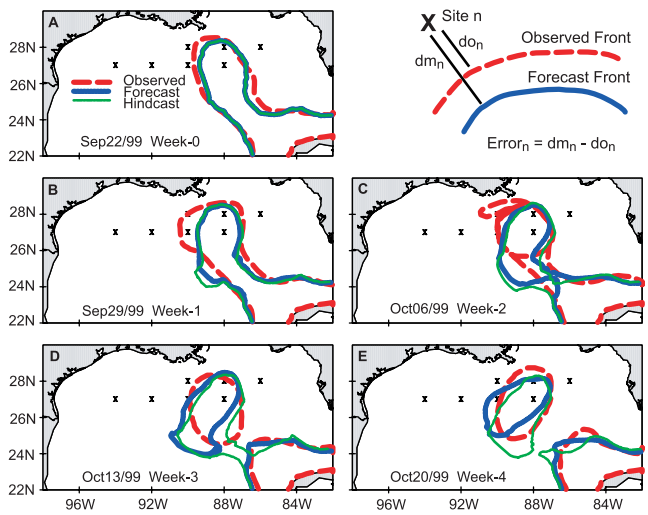


**Figure 4.** Observed (red), forecast (blue) and hindcast (green) frontal positions for Case 2 period Sep/22–Oct/20/1999. Model fronts are determined from the 18°C isotherm at $z = -200$ m. Crosses "X" show the 7 sites from Figure 1. Inset on top right shows schematics of observed and forecast fronts, shortest frontal distances, $dm_n$ and $do_n$, from the site "$n$" and error definition.

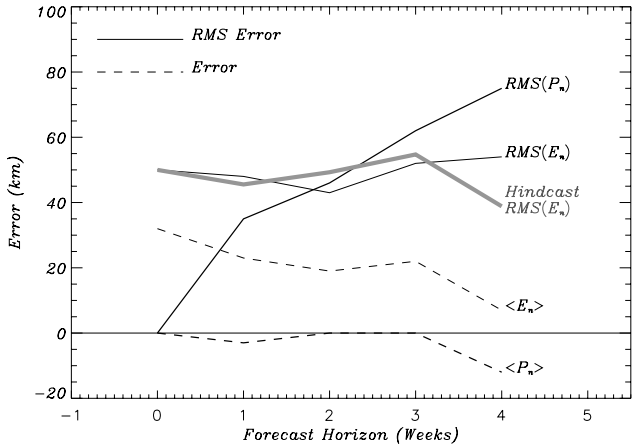


**Figure 5.** Overall forecast and persistence errors, $\langle E_n \rangle$ and $\langle P_n \rangle$, respectively, and their corresponding root-mean-square values $RMS(E_n)$ and $RMS(P_n)$, as functions of the forecast horizon: week-0 through week-4. The thick gray curve is hindcast *RMS* error. See text for details.

skill. However, care must be taken to interpret the results. The $\langle P_n \rangle$ is small through the 4-week forecast horizon due to cancellation of errors primarily amongst the west-east stations as Eddy-J moved westward (as may be shown in the case of steady westward translation of the eddy). Such fortuitous cancellations make $\langle P_n \rangle$ unsuitable as a gauge against which $\langle E_n \rangle$ is assessed. The negative $\langle P_n \rangle$ indicates a bias primarily due to the eddy's southward drift during later test periods (after Case#4), especially when Eddy-J drifted to the southwestern Gulf and the Loop Current retracted (Figure 1). The $P_n$ error itself is large in magnitude, as indicated by the $RMS(P_n)$ curve which increases with forecast horizon, to about 75 km at week-4. The positive $\langle E_n \rangle \approx 20$ km means that on average the forecast front is farther from a site than the observed. This bias is consistent with shift in positions ($15 \sim 25$ km estimated previously) of near-surface (observed) and sub-surface (forecast) fronts. (This presumes also that the majority of the sites are most of the time outside the fronts. This was found to be the case (Figure 1).)

## 5. Discussions and Conclusions

[14] Figure 5 shows that $RMS(E_n)$ beats $RMS(P_n)$ beyond week-2, and indicates that PROFS has some skills: $RMS(E_n) \approx 30-50$ km and $\langle E_n \rangle \approx 20$ km over a 4-week horizon. The $RMS(E_n)$ in the models selected for the test-forecast exercise (see Introduction) are as large as 150 km and the $\langle E_n \rangle \approx \pm 60$ km. These errors are in part due to the ambiguity in comparing surface and sub-surface fronts, which would decrease $\langle E_n \rangle$ by about 15 km, reducing (magnifying) errors in models with positive (negative) $\langle E_n \rangle$. However, that the forecast $RMS(E_n)$ (for PROFS) remains relatively flat with time (Figure 5) suggests that the bulk of the errors are due to the initial (hindcast) fields. The hindcast $RMS(E_n)$ is also included in Figure 5 and affirms this inference. The two curves are statistically not different from each other. Figure 5 indicates that the forecast begins to deteriorate beyond week 3, thus suggesting a model predictability of $3 \sim 4$ weeks. Future work should focus on better assimilation (initialization) schemes, using data other than satellite (e.g. drifters), as well as on improving resolution (physics).

[15] **Acknowledgments.** Supports by the Deepstar and the Minerals Management Service (for PROFS development) are gratefully acknowledged. LYO and TE are also grateful to supports from the Office of Naval Research.

## References

Biggs, D. C., G. S. Fargion, P. Hamilton, and R. R. Leben (1996), Cleavage of a Gulf of Mexico loop current eddy by a deep water cyclone, *J. Geophys. Res.*, *101*, 20,629–20,642.

Blumberg, A. F., and G. L. Mellor (1987), A description of a three-dimensional coastal ocean circulation model, in *Three-Dimensional Coastal ocean Models*, *Coastal and Estuarine Sci.*, vol. 4, edited by N. S. Heaps, pp. 1–16, AGU, Washington, D. C.

Chelton, D. B., R. A. Deszoeke, M. G. Schlax, K. E. Naggar, and N. Siwertz (1998), Geographical variability of the first baroclinic Rossby radius of deformation, *J. Phys. Oceanogr.*, *28*, 433–460.

Cooper, C., G. Z. Forristall, and T. M. Joyce (1990), Velocity and hydrographic structure of two Gulf of Mexico warm-core rings, *J. Geophys. Res.*, *95*, 1663–1679.

Elliott, B. A. (1982), Anticyclonic rings in the Gulf of Mexico, *J. Phys. Oceanogr.*, *12*, 1292–1309.

Ezer, T., D.-S. Ko, and G. L. Mellor (1992), Modeling and forecasting the Gulf Stream, *Mar. Technol. Soc. J.*, *26*, 5–14.

Fan, S. J., L.-Y. Oey, and P. Hamilton (2004), Assimilation of drifters and satellite data in a circulation model of the northeastern Gulf of Mexico, *Cont. Shelf Res.*, *24*(9), 1001–1013.

Forristall, G. Z., K. J. Schaudt, and C. K. Cooper (1992), Evolution and kinematics of a loop current eddy in the Gulf of Mexico during 1985, *J. Geophys. Res.*, *97*, 2173–2184.

Hamilton, P., T. J. Berger, and W. Johnson (2002), On the structure and motions of cyclones in the northern Gulf of Mexico, *J. Geophys. Res.*, *107*(C12), 3208, doi:10.1029/1999JC000270.

Lewis, J. K., and A. D. Kirwan Jr. (1987), Genesis of a Gulf of Mexico ring as determined from kinematic analyses, *J. Geophys. Res.*, *92*, 11,727–11,740.

Mellor, G. L., and T. Ezer (1991), A Gulf Stream model and an altimetry assimilation scheme, *J. Geophys. Res.*, *96*, 8779–8795.

Oey, L.-Y. (1998), Eddy energetics in the Faroe-Shetland Channel: A model resolution study, *Cont. Shelf Res.*, *17*, 1929–1944.

Oey, L.-Y., H.-C. Lee, and W. J. Schmitz Jr. (2003), Effects of winds and Caribbean eddies on the frequency of loop current eddy shedding: A numerical model study, *J. Geophys. Res.*, *108*(C10), 3324, doi:10.1029/2002JC001698.

Vidal, V. M. V., F. V. Vidal, and J. M. Perez-Molero (1992), Collision of a loop current anticyclonic ring against the continental slope of the western Gulf of Mexico, *J. Geophys. Res.*, *97*, 2155–2172.

Vukovich, F. M., and G. A. Maul (1985), Cyclonic eddies in the eastern Gulf of Mexico, *J. Phys. Oceanogr.*, *15*, 105–117.

Walpert, J. N., N. L. Guinasso Jr., F. J. Kelly, L. L. Lee III, O. Wang, and S. DiMarco (2004), 1999 ADCP and XBT surveys of eddy juggernaut in the Gulf of Mexico, technical report to Eddy Joint Industry Project, Geochem. and Environ. Res. Group, Texas A&M Univ., College Station, Tex.

Welsh, S. E., and M. Inoue (2000), Loop current rings and deep circulation in the Gulf of Mexico, *J. Geophys. Res.*, *105*, 16,951–16,959.

Willems, R. C., S. M. Glenn, M. F. Crowley, P. Malanotte-Rizzoli, R. E. Young, T. Ezer, G. L. Mellor, H. G. Arango, A. R. Robinson, and C.-C. A. Lai (1994), Experiment evaluates ocean models and data assimilation in the Gulf Stream, *Eos Trans. AGU*, *75*(34), 385, 391, 394.

C. Cooper, Chevron-Texaco, San Ramon, CA 94583, USA.

S. DiMarco, Department of Oceanography, Texas A&M University, College Station, TX 77843-3146, USA.

T. Ezer and L.-Y. Oey, Department of Atmospheric and Oceanic Sciences, Princeton University, Princeton, NJ 08544, USA. (lyo@princeton.edu)

S. Fan, Stevens Institute of Technology, Hoboken, NJ 07030, USA.

G. Forristall, Forristall Ocean Engineering, Inc., Camden, ME 04843, USA.